

1 **Multiwavelength Observations of The TeV Binary LS I +61° 303**
2 **with VERITAS, Fermi-LAT and Swift-XRT During a TeV**
3 **Outburst**

4 E. Aliu¹ S. Archambault², B. Behera³, K. Berger⁴, M. Beilicke⁵, W. Benbow⁶, R. Bird⁷,
5 A. Bouvier⁸, V. Bugaev⁵, M. Cerruti⁶, X. Chen^{3,9}, L. Ciupik¹⁰, M. P. Connolly¹¹, W. Cui¹²,
6 J. Dumm¹³, A. Falcone¹⁴, S. Federici^{3,9}, Q. Feng¹², J. P. Finley¹², P. Fortin⁶, L. Fortson¹³,
7 A. Furniss⁸, N. Galante⁶, G. H. Gillanders¹¹, S. Griffin², S. T. Griffiths¹⁵, J. Grube¹⁰,
8 G. Gyuk¹⁰, D. Hanna², J. Holder⁴, G. Hughes³, T. B. Humensky¹, P. Kaaret¹⁵,
9 M. Kertzman¹⁶, Y. Khassen⁷, D. Kieda¹⁷, F. Krennrich¹⁸, M. J. Lang¹¹, G. Maier³,
10 P. Majumdar^{19,20}, S. McArthur²¹, A. McCann²², P. Moriarty²³, R. Mukherjee¹,
11 A. O’Faoláin de Bhróithe⁷, R. A. Ong¹⁹, A. N. Otte²⁴, N. Park²¹, J. S. Perkins²⁵,
12 M. Pohl^{3,9}, A. Popkow¹⁹, H. Prokoph³, J. Quinn⁷, K. Ragan², J. Rajotte², G. Ratliff¹⁰,
13 P. T. Reynolds²⁶, G. T. Richards²⁴, E. Roache⁶, G. H. Sembroski¹², F. Sheidaei^{17,*},
14 C. Skole³, A. W. Smith^{17,*}, D. Staszak², I. Telezhinsky^{3,9}, J. Tyler², A. Varlotta¹²,
15 S. Vincent³, S. P. Wakely²¹, T. C. Weekes⁶, A. Weinstein¹⁸, R. Welsing³, A. Zajczyk⁵
16 B. Zitzer²⁷

*Corresponding Authors: aw.smith@utah.edu, sheidaei@physics.utah.edu

¹Physics Department, Columbia University, New York, NY 10027, USA

²Physics Department, McGill University, Montreal, QC H3A 2T8, Canada

³DESY, Platanenallee 6, 15738 Zeuthen, Germany

⁴Department of Physics and Astronomy and the Bartol Research Institute, University of Delaware, Newark, DE 19716, USA

⁵Department of Physics, Washington University, St. Louis, MO 63130, USA

⁶Fred Lawrence Whipple Observatory, Harvard-Smithsonian Center for Astrophysics, Amado, AZ 85645, USA

⁷School of Physics, University College Dublin, Belfield, Dublin 4, Ireland

⁸Santa Cruz Institute for Particle Physics and Department of Physics, University of California, Santa Cruz, CA 95064, USA

⁹Institute of Physics and Astronomy, University of Potsdam, 14476 Potsdam-Golm, Germany

¹⁰Astronomy Department, Adler Planetarium and Astronomy Museum, Chicago, IL 60605, USA

¹¹School of Physics, National University of Ireland Galway, University Road, Galway, Ireland

¹²Department of Physics, Purdue University, West Lafayette, IN 47907, USA

¹³School of Physics and Astronomy, University of Minnesota, Minneapolis, MN 55455, USA

¹⁴Department of Astronomy and Astrophysics, 525 Davey Lab, Pennsylvania State University, University Park, PA 16802, USA

¹⁵Department of Physics and Astronomy, University of Iowa, Van Allen Hall, Iowa City, IA 52242, USA

¹⁶Department of Physics and Astronomy, DePauw University, Greencastle, IN 46135-0037, USA

¹⁷Department of Physics and Astronomy, University of Utah, Salt Lake City, UT 84112, USA

¹⁸Department of Physics and Astronomy, Iowa State University, Ames, IA 50011, USA

¹⁹Department of Physics and Astronomy, University of California, Los Angeles, CA 90095, USA

²⁰Saha Institute of Nuclear Physics, Kolkata 700064, India

²¹Enrico Fermi Institute, University of Chicago, Chicago, IL 60637, USA

²²Kavli Institute for Cosmological Physics, University of Chicago, Chicago, IL 60637, USA

²³Department of Life and Physical Sciences, Galway-Mayo Institute of Technology, Dublin Road, Galway, Ireland

²⁴School of Physics and Center for Relativistic Astrophysics, Georgia Institute of Technology, 837 State Street NW, Atlanta, GA 30332-0430

²⁵N.A.S.A./Goddard Space-Flight Center, Code 661, Greenbelt, MD 20771, USA

17 **ABSTRACT**

18 We present the results of a multiwavelength observational campaign on the
 TeV binary system LS I +61° 303 with the VERITAS telescope array (>200
 GeV), Fermi-LAT (0.3-300 GeV), and Swift-XRT (2-10 keV). The data were
 taken from December 2011 through January 2012 and show a strong detection in
 all three wavebands. During this period VERITAS obtained 24.9 hours of quality
 selected livetime data in which LS I +61° 303 was detected at a statistical sig-
 nificance of 11.9σ . These TeV observations show evidence for nightly variability
 in the TeV regime at a post-trial significance of 3.6σ . The combination of the
 simultaneously obtained TeV and X-ray fluxes do not demonstrate any evidence
 for a correlation between emission in the two bands. For the first time since the
 launch of the Fermi satellite in 2008, this TeV detection allows the construction
 of a detailed MeV-TeV spectral energy distribution from LS I +61° 303. This
 spectrum shows a distinct cutoff in emission near 4 GeV, with emission seen by
 the VERITAS observations following a simple power-law above 200 GeV. This
 feature in the spectrum of LS I +61° 303, obtained from overlapping observa-
 tions with Fermi-LAT and VERITAS, may indicate that there are two distinct
 populations of accelerated particles producing the GeV and TeV emission.

19 *Subject headings:*

20 **1. Introduction**

21 The high-mass X-ray binary LS I +61° 303 is perhaps the most studied member of a
 22 surprisingly small class of X-ray binary systems which are also known sources of TeV emis-
 23 sion. Despite many years of observations across the electromagnetic spectrum, the system
 24 remains, in some respects, poorly characterized. Known to be the pairing of a massive B0 Ve
 25 star and a compact object of unknown nature (Casares et al. 2005; Hutchings & Crampton
 26 1981), LS I +61° 303 has been known historically for its energetic outbursts at radio, X-
 27 ray, GeV, and TeV wavelengths (Abdo et al. 2009a; Acciari et al. 2008; Albert et al. 2006;
 28 Gregory 2002; Greiner & Rau 2001; Harrison et al. 2000; Zhang et al. 2010), all of these

²⁶Department of Applied Physics and Instrumentation, Cork Institute of Technology, Bishopstown, Cork, Ireland

²⁷Argonne National Laboratory, 9700 S. Cass Avenue, Argonne, IL 60439, USA

29 showing correlation with the 26.5 day orbital cycle of the compact object. Radial velocity
 30 measurements show the orbit to be elliptical ($e = 0.537 \pm 0.034$), with periastron passage
 31 occurring around phase $\phi = 0.275$, apastron passage at $\phi = 0.775$, superior conjunction at
 32 $\phi = 0.081$ and inferior conjunction at $\phi = 0.313$ (Aragona et al. 2009). Although it should
 33 be noted that all of the orbital parameters of LS I +61° 303 are subject to some uncertainty
 34 as the inclination of the system is not precisely known.

35 Observations in the non-thermal regime have managed to illustrate some key phenom-
 36 ena. Extensive observations by both RXTE and Swift-XRT have provided a wealth of X-ray
 37 data which show a regular emission period consistent with the orbital period (Smith et al.
 38 2009; Esposito et al. 2007). The modulation of this X-ray peak is seen on multiple timescales,
 39 from individual orbits up to several years; most importantly, a modulation on a ~ 4.5 year
 40 timescale (Li et al. 2012; Chernyakova et al. 2012) has been observed in the hard X-ray
 41 band, reminiscent of the well known 4.5 year modulation of the radio period (Gregory 2002).
 42 However, a definitive link between the particle acceleration processes producing the radio
 43 emission and those producing the X-ray emission is still lacking. An additional feature of the
 44 system is the possible association of short (< 0.1 s), high luminosity X-ray bursts from the
 45 system (Pasquale et al. 2008; Burrows 2012) which have been interpreted as the result of the
 46 emission from a high magnetic field neutron star (A. Papitto 2012). Further observations
 47 of such behavior from the system in the X-ray band, definitively linked to LS I +61° would
 48 solidify this association.

49 In the GeV band, LS I +61° 303 was one of the few non-pulsar galactic objects firmly
 50 identified in the initial Fermi-LAT Bright Source List with an average flux of $(0.82 \pm 0.03_{stat} \pm$
 51 $0.07_{syst}) \times 10^{-6} \text{ } \gamma \text{ cm}^{-2} \text{ s}^{-1}$ above 100 MeV (Abdo et al. 2009a). The spectrum showed an
 52 exponential cutoff at $6.3 \pm 1.1_{stat} \pm 0.4_{sys}$ GeV and a photon index of $\Gamma = 2.21 \pm 0.04_{stat} \pm$
 53 0.06_{sys} . In the first 8 months of LAT data, the source demonstrated a clear modulation of
 54 GeV emission with a period of ~ 26.5 days, compatible with the radio period. The highest
 55 GeV fluxes were measured around phase $\phi = 0.4$, close to periastron. However, subsequent
 56 analysis of ~ 4.5 years of Fermi-LAT data shows clear evidence for long term variability of the
 57 mean orbital flux along with the apparent disappearance of its previously observed orbital
 58 modulation (Hadasch et al. 2012). This long term variability has recently been elucidated
 59 in Hadasch et al. (2013), where the Fermi-LAT collaboration shows a detection of the ~ 4.5
 60 year modulation of the GeV flux around apastron, consistent with the modulation seen in
 61 both radio and X-rays.

62 As a TeV source, the system has presented puzzling behavior. Initial detections in 2006-
 63 2007 by both the VERITAS and MAGIC collaborations (Albert et al. 2006; Acciari et al.
 64 2008) over many orbital cycles showed the source to be a variably bright TeV source,

65 with emission peaking around apastron passage. Subsequent observations in 2008-2010
66 (Acciari et al. 2011) showed no evidence for emission during these previously detected phases,
67 instead only detecting the source at a lower TeV flux near the periastron passage of a single
68 orbit. The connection between the observed emission in different energy bands is not clear;
69 initial detections of a correlation between the TeV and X-ray fluxes (Albert et al. 2012) were
70 not seen in later observations. Additionally, previous observations have not shown the GeV
71 and TeV emission from the system to be strongly correlated either (Acciari et al. 2011).

72 As is the case with many TeV sources, the models to explain observed emission consist
73 of both leptonic (inverse Compton scattering) and hadronic (pion decay resulting from rela-
74 tivistic proton interactions) variations. LS I +61° 303 is certainly no different in this respect,
75 however, the confusion between emission models is compounded by an ambiguity in what
76 type of engine actually powers the particle acceleration. LS I +61° 303 was originally thought
77 to be a microquasar system due to the observation of what appeared to be extended radio
78 jets (Massi et al. 2001). In this scenario, emission from the system is powered by a variably
79 fed accretion disk which, in turn, powers a relativistic jet. The variability observed across
80 the spectrum would then be explained by the accretion disk’s exposure to varying levels of
81 the strong stellar wind common to Be star systems. This model (under the assumption of
82 basic Bondi-Hoyle accretion) would then predict non-thermal emission in the various bands
83 to be coupled (in the simplest scenario) with the maximum flux occurring near periastron
84 passage where the density of the stellar material is greatest. While this appears to be true
85 sometimes in the GeV regime, it is not true in the TeV regime where emission is typically
86 at a maximum near apastron passage.

87 However, the existence of a radio jet (and the validity of using a microquasar scenario)
88 was called into question by high resolution VLBA imaging which observed what appeared
89 to be the cometary emission from the interaction between a pulsar wind and the wind of the
90 stellar companion (Dhawan et al. 2006). In this scenario (where the emission is powered by
91 a shock front between the two winds) the variability would also result from varying levels of
92 stellar wind density. However, in this model the emission in the various bands is decoupled
93 by both the magnetic field strength at the shock and “stand off distance” (distance from the
94 shock to the pulsar) changing as function of orbit. The change in these two quantities would
95 dictate both cooling mechanisms and acceleration parameters, thus changing the relative
96 intensities of emission between bands.

97 It should be pointed out that neither of these models can explain all of the observed
98 emission variability in the system (for instance, the VERITAS detection of TeV emission
99 far away from apastron passage). Additionally, since neither pulsations nor an accretion-
100 like X-ray spectrum have yet to be observed in the system, current observations have not

101 yielded a definitive answer to whether the system harbors a pulsar or black hole and both
 102 theoretical frameworks used to describe this system are still lacking strong constraints. What
 103 is clear however, is that the simplest version of either model will not adequately explain the
 104 observations. For example, both photon-photon absorption and line-of-sight effects almost
 105 certainly have to be taken into account when accounting for the observed variability. For
 106 examples of more recently advanced observations and models, see Zabalza et al. (2013),
 107 Torres et al. (2012) (binary pulsar model) and Zimmerman & Torres (2012) (microquasar
 108 model).

109 Determining the correct physical model for this source requires additional dedicated
 110 observations across the multiwavelength spectrum. In this work we detail the multiwave-
 111 length campaign on LS I +61° 303 incorporating both contemporaneous and simultaneous
 112 observations in the X-ray (Swift-XRT), GeV (Fermi-LAT), and TeV (VERITAS) regimes.
 113 This campaign was taken during a relatively strong period of emission in the TeV regime,
 114 and stands as the first time that simultaneous GeV/TeV have been available during a high
 115 TeV state. During this high state, VERITAS detected marginal evidence for nightly vari-
 116 ability in the system as well as a lack of strong correlated emission between the TeV flux
 117 and X-ray/GeV fluxes. Additionally, the spectral energy distribution obtained during these
 118 observations reveals a puzzling lack of detected emission between 30 and 200 GeV which
 119 makes the characterization of the gamma-ray emission non-trivial.

120 2. VERITAS Observations

121 The VERITAS array (Holder et al. 2008) of imaging atmospheric Cherenkov telescopes
 122 (IACTs), located in southern Arizona (1.3 km a.s.l., 31°40'30" N, 110°57'07" W), began 4-
 123 telescope array observations in September 2007. The array is composed of four 12m diameter
 124 telescopes, each with a Davies-Cotton tessellated mirror structure of 345 12m focal length
 125 hexagonal mirror facets (total mirror area of 110 m²). Each telescope focuses Cherenkov
 126 light from particle showers onto its 499-pixel photomultiplier tube camera. Each pixel has a
 127 field of view of 0.15°, resulting in a camera field of view of 3.5°. VERITAS has the capability
 128 to detect and measure gamma rays in the 100 GeV to 30 TeV energy regime with an energy
 129 resolution of 15-20% and an angular resolution of <0.1° on an event by event basis.

130 VERITAS observed LS I +61° 303 beginning in early December 2011 (MJD 55911)
 131 until late January 2012 (MJD 55497), acquiring a total of 24.5 hours of quality selected,
 132 live-time observations. These observations provided detailed (although uneven) sampling
 133 of the phase bins $\phi=0.45-0.05$ of the binary orbit. Figure 1 shows the source light curve
 134 binned by both MJD and orbital phase. During the orbital phase regions of 0.5-0.8, the

135 source was highly active, presenting a flux of $5\text{--}15 \times 10^{-12} \gamma\text{s cm}^{-2}\text{s}^{-1}$ above 350 GeV, or
 136 approximately 5–15% of the Crab Nebula flux in the same energy regime. For the entire
 137 24.5 hour observation, VERITAS detected an excess of 791 events from LS I +61° 303,
 138 equivalent to a detection at the 11.9σ significance level. The data are used to create a
 139 differential energy spectrum from 0.2–5 TeV which is reasonably fit by a power-law ($\chi^2/\text{n.d.f}$
 140 $= 1.1/5$) described by $(1.37 \pm 0.14_{\text{stat}}) \times 10^{-12} \times (\frac{E}{1\text{TeV}})^{-2.59 \pm 0.15_{\text{stat}}} \gamma\text{s TeV}^{-1} \text{ cm}^{-2} \text{ s}^{-1}$. A
 141 comparison of this spectrum with those obtained by previous measurements at different
 142 flux levels (Aleksic et al. 2012; Acciari et al. 2008) shows no indication for variability in the
 143 spectral slope from the source across a wide range of flux levels (see Figure 2).

144 The observations of LS I +61° 303 taken in 2011 also display an indication that the
 145 source may be variable in the TeV regime on a timescale much shorter than previously
 146 observed. While LS I +61° 303 is known to be a variable TeV source on the timescale of
 147 a single orbital period, the 2011 VERITAS observations indicate that the source may be
 148 variable on a nightly timescale. To test this hypothesis, we proceed by collecting the nightly
 149 absolute fluxes (Figure 1) and finding the pairs of observations which are separated by 1
 150 day. Nine such pairs of observations exists within the 2011 observations and their fluxes are
 151 shown in Table 1. To test for variability on a nightly timescale we choose to test against the
 152 null hypothesis that, given a pair of nightly separated fluxes (F_1, F_2), F_2 was significantly
 153 larger than F_1 (as well as the inverse hypothesis). Assuming that both the source fluxes and
 154 errors are normally distributed, we construct the 2-dimensional Gaussian function:

$$G(x, y) = \frac{1}{2\pi\sigma_1\sigma_2} e^{-\frac{(x-F_1)^2}{2\sigma_1^2} - \frac{(y-F_2)^2}{2\sigma_2^2}} \quad (1)$$

155 where σ represents the errors on the measured fluxes, and x and y are both flux space
 156 variables. Within this parametrization, a constant flux from night to night is represented by
 157 the function $y=x$. The probabilities that F_2 was greater than F_1 (or vice versa) can then be
 158 obtained by examining the integral:

$$\int_{-\infty}^{+\infty} dx \int_x^{+\infty} G(x, y) dy \quad (2)$$

159 The resulting probabilities for $F_1 >, < F_2$ (Table 1) show marginal evidence that the
 160 source is variable on a nightly timescale. The observations taken on MJD 55918/55919 and
 161 MJD 55944/55945 show evidence for a flux decrease at the 2.7σ and 3.6σ significance level
 162 respectively. These significances are post-trials, accounting for nine trials (one trial for each
 163 nightly pair tested). We note that this analysis does not search for evidence of variability
 164 at any timescales other than the nightly timescale. The flux differences present evidence for

165 the TeV flux falling on a nightly timescale. However, we did not observe an increase in TeV
 166 flux on this same short timescale.

167 3. Multiwavelength Data

168 3.1. *Swift*-XRT

169 The *Swift* X-ray Telescope (XRT) data (Burrows et al. 2005) were reduced using the
 170 HEASoft 6.12 package. Event files are calibrated and cleaned following the standard filtering
 171 criteria using the xrtpipeline task and applying the most recent Swift XRT calibration files.
 172 All data were taken in photon counting (PC) mode, with grades 0-12 selected over the energy
 173 range 0.3-10 keV. Since the count rate was below 0.5 counts s⁻¹ for all data, no evidence
 174 for photon pile-up in the core of the point-spread function (PSF) is evident. The source
 175 events are extracted from a circular region of radius of 30 pixels (47.2 arcsec). Background
 176 counts are extracted from a 40 pixel radius circle in a source-free region. Ancillary response
 177 files are generated using the xrtmkarf task, with corrections applied for the PSF losses and
 178 CCD defects. The latest response matrix from the XRT calibration files is applied. To
 179 ensure valid χ^2 minimization statistics during spectral fitting, the extracted XRT energy
 180 spectra are rebinned to contain a minimum of 20 counts in each bin. Spectral analysis is
 181 performed with XSPEC 12.7. An absorbed power-law model, including the phabs model for
 182 the photoelectric absorption, is fit to each spectrum. A fixed column density is applied with
 183 an N_H of 6.1×10^{21} cm⁻² (Rea et al. 2010). The spectral index of the source varied from -2.5
 184 to -1.1 with reduced χ^2 values ranging from 0.2 to 1.6. As observed in Smith et al. (2009),
 185 the data show evidence for a correlation between the spectral index of the source and the
 186 0.2-10 keV flux, with a Pearson correlation coefficient derived of 0.8 ± 0.1 .

187 The overall Swift-XRT light curve was extracted in the energy range of 2-10 keV and is
 188 shown in Figure 1. There were eight Swift-XRT observations that were taken simultaneously
 189 with VERITAS data (shown by grey bars in Figure 1). In order to compare the VERITAS
 190 flux measurements with previous X-ray-TeV correlation studies, the 350 GeV fluxes were
 191 interpolated to 300 GeV fluxes using the fitted spectral index of -2.59 derived from the current
 192 observations. Both the VERITAS/Swift observations taken in 2011/2012 as well as archival
 193 VERITAS and MAGIC measurements (Acciari et al. 2011) are shown in Figure 3. The
 194 correlation factor derived from the 2011/2012 observations was 0.36 ± 0.32 , consistent with
 195 two uncorrelated datasets. Including all simultaneous X-ray/TeV pointings from VERITAS
 196 and MAGIC results in a correlation coefficient of 0.33 ± 0.14 , which is consistent with no
 197 correlation.

MJD	Flux (>350 GeV) $\times 10^{-12} \gamma \text{s cm}^{-2} \text{s}^{-1}$	$p(\mathbf{F}_1 > \mathbf{F}_2)$ (σ)	$p(\mathbf{F}_2 > \mathbf{F}_1)$ (σ)
55911	-1.5 ± 1.8	$< 10^{-5}$ ($< 0.1\sigma$)	
55912	-1.02 ± 2.0		0.18 (0.23 σ)
55918	13.5 ± 2.8	0.99 (2.72σ)	
55919	3.7 ± 1.3		$< 10^{-5}$ ($< 0.1\sigma$)
55919	3.7 ± 1.3	0.76 (1.17 σ)	
55920	-0.77 ± 2.0		$< 10^{-5}$ ($< 0.1\sigma$)
55920	-0.77 ± 2.0	3.9×10^{-3} ($< 0.1\sigma$)	
55921	-1.02 ± 2.0		7.6×10^{-4} ($< 0.1\sigma$)
55924	1.3 ± 1.8	$< 10^{-5}$ ($< 0.1\sigma$)	
55925	7.2 ± 2.8		0.69 (1.01 σ)
55943	18.6 ± 3.3	1.6×10^{-3} ($< 0.1\sigma$)	
55944	18.6 ± 2.8		1.9×10^{-3} ($< 0.1\sigma$)
55944	18.6 ± 2.8	0.99 (3.57σ)	
55945	4.8 ± 2.1		$< 10^{-5}$ ($< 0.1\sigma$)
55945	4.8 ± 2.1	7.4×10^{-3} ($< 0.1\sigma$)	
55946	4.1 ± 2.4		4.0×10^{-4} ($< 0.1\sigma$)
55946	4.1 ± 2.4	$< 10^{-5}$ ($< 0.1\sigma$)	
55947	13.7 ± 5.9		0.47 (0.63 σ)

Table 1: The probabilities for both the flux increase and decrease per each pair of nightly separated fluxes. All probabilities shown are post-trials, accounting for nine trials (nine pairs of fluxes). All errors quoted are statistical only.

3.2. Fermi-LAT

198

199 *Fermi*-LAT (Atwood et al. 2009) analysis was performed on all available photons in the
 200 0.3-300 GeV band obtained between December 1 2011 (MJD 55896) and February 1 2012
 201 (MJD 55958), in order to overlap as closely as possible with the VERITAS observations. The
 202 data were analyzed using Science Tools version v9r31p1, available from the Fermi Science
 203 Support Center (FSSC)¹. Standard data quality cuts for Pass 7 event reconstruction were
 204 applied as recommended by the FSSC, with only “source” (class 2) events being used for
 205 analysis. Other standard cuts were also applied (e.g. zenith angle larger than 100° in order
 206 to reduce the contamination from atmospheric secondary gamma rays from near the Earth’s
 207 limb (Abdo et al. 2009b)).

208 The LAT light curve was produced using the python likelihood tools and scripts available
 209 from the FSSC². A region of interest (ROI) of 10° was chosen and a model file incorporating
 210 all 2FGL sources within a region of 15° was used for the initial fit. In this fit, all source
 211 showing a test statistic (TS) value of less than 1 for the data interval chosen were excluded.
 212 Additionally, all source more than 5° from the center of the ROI had fixed parameters in the
 213 model fitting. The resulting model was used to produce the daily binned lightcurve (shown in
 214 Figure 1), by fixing all 2FGL source model parameters (with the exception of LS I +61° 303
 215 and the nearby pulsar 2FGL J0248.1+6021). To test for any correlation between the GeV
 216 and TeV flux, a correlation coefficient between the overlapping observations is calculated,
 217 with a coefficient of $r=0.1\pm 0.3$, consistent with two uncorrelated datasets (see Figure 4).

218 For spectral analysis, a binned maximum-likelihood method (`gtlike`) was used with an
 219 energy dependent ROI ranging from 2° to 10°. In order to determine the background, the
 220 2FGL catalog (Nolan et al. 2012) was used to account for the emission from all sources within
 221 a radius ranging between 3° to 15° (also a function of energy). The spectrum is satisfactorily
 222 fit (reduced χ^2 value of 1.97 with 5 degrees of freedom) by a power law with exponential
 223 cutoff of the form $A \times \frac{E}{1\text{MeV}}^{-\Gamma} \times \exp^{-(E/E_{cutoff})}$, with $A = (2.5 \pm 0.9) \times 10^{-4} \text{ } \gamma_s \text{ MeV}^{-1} \text{ cm}^{-2}$
 224 s^{-1} , $\Gamma = 2.13 \pm 0.06$, and $E_{cutoff} = 3.98 \pm 0.42 \text{ GeV}$ (see Figure 5). When comparing this
 225 spectrum to the one observed by VERITAS during contemporaneous observations, it is clear
 226 that the emission seen by Fermi-LAT experiences a dramatic fall off that is not observed in
 227 the TeV regime (see Figure 5). Since VERITAS observed the source at relatively large zenith
 228 angles (30°-35°), the energy threshold of the TeV observations do not allow for a detailed
 229 examination of the 100-200 GeV energy range.

¹<http://fermi.gsfc.nasa.gov/ssc/>

²<http://fermi.gsfc.nasa.gov/ssc/data/analysis/user/>

4. Summary and Discussion

230

231 We have presented the results of a comprehensive multiwavelength campaign of the
 232 TeV binary LS I +61° 303 using VERITAS, Swift-XRT, and Fermi-LAT observations. The
 233 source was detected strongly in the TeV regime while not showing a significant correlation
 234 with the observed emission in the X-ray or MeV-GeV regimes. The VERITAS differential
 235 energy spectrum obtained from these observations is well fit by a power law with spectral
 236 index consistent with previously published observations. The combination of the differential
 237 energy spectra obtained by both Fermi-LAT and VERITAS during the same time period
 238 reveals a puzzling lack of detected emission in the 1-200 GeV range. While the observation
 239 of this apparent discontinuity is not new (for example, Hadasch et al. (2012)) the previous
 240 GeV-TeV multi wavelength SEDs of LS I +61° 303 have, up until now, been constructed
 241 with data taken from various epochs. The observations detailed here represent the first time
 242 that a contemporaneous SED has been constructed with Fermi-LAT and IACTs since the
 243 launch of Fermi in 2008. The distinctive cutoff seen in the Fermi-LAT data, coupled with
 244 the significant detection of emission in the >200 GeV VERITAS energy range during the
 245 contemporaneous observations detailed in this work indicate that the observed emission in the
 246 Fermi-LAT/VERITAS energy ranges is produced by two separate populations of particles.
 247 While we allow for the possibility that short term spectral variability in the Fermi-LAT
 248 energy regime could, in principle, produce a direct connection to the VERITAS TeV points,
 249 we consider such behavior unlikely given the spectral stability of the source in the Fermi-LAT
 250 regime (Abdo et al. 2009a).

251 Given that the GeV spectral cutoff observed in LS I +61° 303 is strongly reminiscent of
 252 the typical cutoff shape seen in known Fermi-LAT pulsars, it is natural to suspect that emis-
 253 sion in the system is indeed powered by an energetic pulsar. This model, as first proposed
 254 in Maraschi & Treves (1981) and later developed and modeled in detail by (Dubus 2006),
 255 explains the observed gamma-ray emission in LS I +61° 303 (as well as other known TeV bina-
 256 ries such as LS 5039 and PSR B1259-63) as being produced by the rotation power of a young
 257 pulsar. The inclusion of a pulsar in the system allows for much more flexibility in producing
 258 disparate populations of energetic particles (as appears to be observationally required in
 259 systems such as LS I +61° 303 and LS 5039) as there can be multiple acceleration regions for
 260 GeV/TeV energy particles: the inner pulsar magnetosphere, the shock interface between the
 261 pulsar and stellar winds (as well as multiple shocks separated by a contact discontinuity, as in
 262 Bednarek (2011)), acceleration within the pulsar wind zone (Sierpowska-Bartosik & Torres
 263 (2008)), and potentially Coriolis effect generated shock fronts on scales much larger than the
 264 binary system (i.e. Zabalza et al. (2013)).

265 If we assume that the TeV emission is produced in the shock interaction between the two

266 winds, and that the GeV emission is produced in a second acceleration region or different seed
 267 particles, then it is possible that the GeV emission might be produced in the inner regions
 268 of the pulsar magnetosphere. The observed GeV variability could then be explained by
 269 absorption effects as the pulsar travels through the varying stellar wind density of the Be star.
 270 This would offer a natural explanation for the lack of GeV emission in the arguably similar
 271 TeV binary system HESS J0632+057; the pulsar beam in that system could be pointed away
 272 from our line of sight. Bednarek (2011) argues against the pulsar magnetosphere being the
 273 source of the GeV emission in the GeV/TeV binary systems, citing the lack of GeV emission
 274 from PSR B 1259-63 away from periastron where absorption effects should not play a strong
 275 role. This is indeed true and would necessitate a different mechanism for GeV emission in
 276 PSR B1259-63; however, given the relative uncertainty in the various physical parameters of
 277 the known TeV binaries, it is entirely possible that different mechanisms for emission could
 278 be at work in the different binary systems.

279 The identification of LS I +61° 303 as a binary pulsar system is certainly not clear. For
 280 instance, despite many extensive searches Cañella et al. (2012); McSwain et al. (2011), no
 281 pulsations have ever been detected, although it is possible that the dense stellar environment
 282 of LS I +61° 303 might preclude such a detection.

283 The observations presented here also reveal the first strong evidence (99.97% confidence)
 284 for nightly variability in the source. If confirmed, this variability can provide crucial con-
 285 straints on the size of the TeV emission region (i.e. the size of possible “clumps” in the wind
 286 for pulsar binary models). Fast variability (\sim second timescale) has already been associated
 287 with LS I +61° 303 in the X-ray regime (Smith et al. 2009; Torres et al. 2010), limiting the
 288 size of the X-ray emission region. Given the source strength of LS I +61° 303 and current
 289 sensitivity of IACT arrays, it is unlikely that such fast variability will be observed by the
 290 current generation of TeV instruments, even if occurring in the source. However, if the TeV
 291 and X-ray emission have a common mechanism, it could be possible to observe variability in
 292 the system on the order of tens of minutes during TeV flaring episodes.

293 These observations, taken in the context of past observations with VERITAS and
 294 MAGIC, also bring up the issue of the possible long-term variability seen in the system.
 295 Observations of this system with TeV instruments have only been taking place since 2006;
 296 while the observations have not been dense enough to make strong statements about the
 297 long term behavior of the source, it would appear that the source may go through a long-
 298 term modulation in the high energy regime. The source was a strong TeV source in 2006/7
 299 (Acciari et al. 2008; Albert et al. 2006), however, its TeV flux appears to have decreased over
 300 the succeeding years (Acciari et al. 2011; Aleksic et al. 2012). The “normal” apastron TeV
 301 emission was markedly quiet, while the source was sporadically detected at near-periastron

302 phases. The VERITAS observations taken in 2011/2012 indicate that the source may have
303 returned to its “normal” emission mode, with strong emission seen near apastron. Further
304 long term observations of LS I +61° 303 with TeV instruments are key to understanding
305 the possible multiyear modulation of the source and (given the lack of detected correlation
306 between TeV emission and other bands) whether or not it is tied to similar emission mod-
307 ulation in radio (Gregory 2002), X-ray (Li et al. 2012; Chernyakova et al. 2012) and GeV
308 gamma-rays (Hadasch et al. 2013).

309 This research is supported by grants from the U.S. Department of Energy Office of
310 Science, the U.S. National Science Foundation and the Smithsonian Institution, by NSERC
311 in Canada, by Science Foundation Ireland (SFI 10/RFP/AST2748) and by STFC in the
312 U.K. We acknowledge the excellent work of the technical support staff at the Fred Lawrence
313 Whipple Observatory and at the collaborating institutions in the construction and operation
314 of the instrument. We thank the Swift Team for scheduling contemporaneous observations
315 and providing data and analysis tools. The authors would also like to thank Jeremy Perkins
316 for his tireless assistance with Fermi-LAT data analysis.

317 REFERENCES

- 318 A. Papitto, D. Torres, N. R. 2012, *The Astrophysical Journal*, 756, 188
- 319 Abdo, A., et al. 2009a, *ApJ*, 701, L123
- 320 —. 2009b, *Phys. Rev. D*, 80, 12
- 321 Acciari, V., et al. 2008, *ApJ*, 679, 1427
- 322 —. 2011, *ApJ*, 738, 3
- 323 Albert, J., et al. 2006, *Science*, 312, 1771
- 324 —. 2012, *ApJ*, 683, 1351
- 325 Aleksic, J., et al. 2012, *ApJ*, 746, 80
- 326 Aragona, C., et al. 2009, *ApJ*, 698, 514
- 327 Atwood, W., et al. 2009, *ApJ*, 697, 1071
- 328 Bednarek, W. 2011, *MNRAS Letters*, 418, 1

- 329 Burrows, D. 2012, GRB Coordinates Network, 12914, 1
- 330 Burrows, D., et al. 2005, Space Sci. Rev., 120, 165
- 331 Cañella, A., et al. 2012, A&A, 543, 122
- 332 Casares, J., et al. 2005, MNRAS, 360, 1105
- 333 Chernyakova, M., et al. 2012, ApJ. Lett., 747, L29
- 334 Dhawan, V., et al. 2006, in Proc. of Microquasars and Beyond: From Binaries to Galaxies, in
335 Proceedings of Science, Como, IT, ed. T. Belloni, p 52
- 336 Dubus, G. 2006, A&A, 3, 801
- 337 Esposito, P., Caraveo, P. A., Pellizzoni, A., Luca, A. D., Gehrels, N., & Marelli, M. A. 2007,
338 A&A, 474, 575
- 339 Gregory, P. 2002, ApJ, 525, 427
- 340 Greiner, J., & Rau, A. 2001, A&A, 375, 145
- 341 Hadasch, D., et al. 2012, ApJ, 749, 1
- 342 —. 2013, Accepted for publication in The Astrophysical Journal Letters, astro-ph/1307.6384
- 343 Harrison, F., et al. 2000, ApJ, 528, 454
- 344 Holder, J., et al. 2008, American Institute of Physics Conference Series, 1085, 657
- 345 Hutchings, J., & Crampton, D. 1981, PASP, 93, 486
- 346 Li, J., et al. 2012, ApJ, 744, L13
- 347 Maraschi, L., & Treves, A. 1981, MNRAS, 194, 1
- 348 Massi, M., et al. 2001, A&A, 376, 217
- 349 McSwain, V., et al. 2011, ApJ, 738, 1
- 350 Nolan, P., et al. 2012, ApJ Supp., 199, 31N
- 351 Pasquale, M. D., et al. 2008, GRB Coordinates Network, 8209, 1
- 352 Rea, N., et al. 2010, MNRAS, 405, 2206
- 353 Sierpowska-Bartosik, A., & Torres, D. 2008, Astroparticle Physics, 30, 239

- 354 Smith, A., Falcone, A., Holder, J., Kaaret, P., Maier, G., & Pandel, D. 2009, *ApJ*, 693, 1621
- 355 Torres, D., Rea, N., & Esposito, P. 2012, *ApJ*, 744, 106
- 356 Torres, D., et al. 2010, *ApJ Lett.*, 719, L104
- 357 Zabalza, V., Bosch-Ramon, V., Aharonian, F., & Khangulyan, D. 2013, *A&A*, 551, A13
- 358 Zhang, S., et al. 2010, *MNRAS*, 408, 642
- 359 Zimmerman, L., & Torres, M. M. 2012, *A&A*, 537, 482

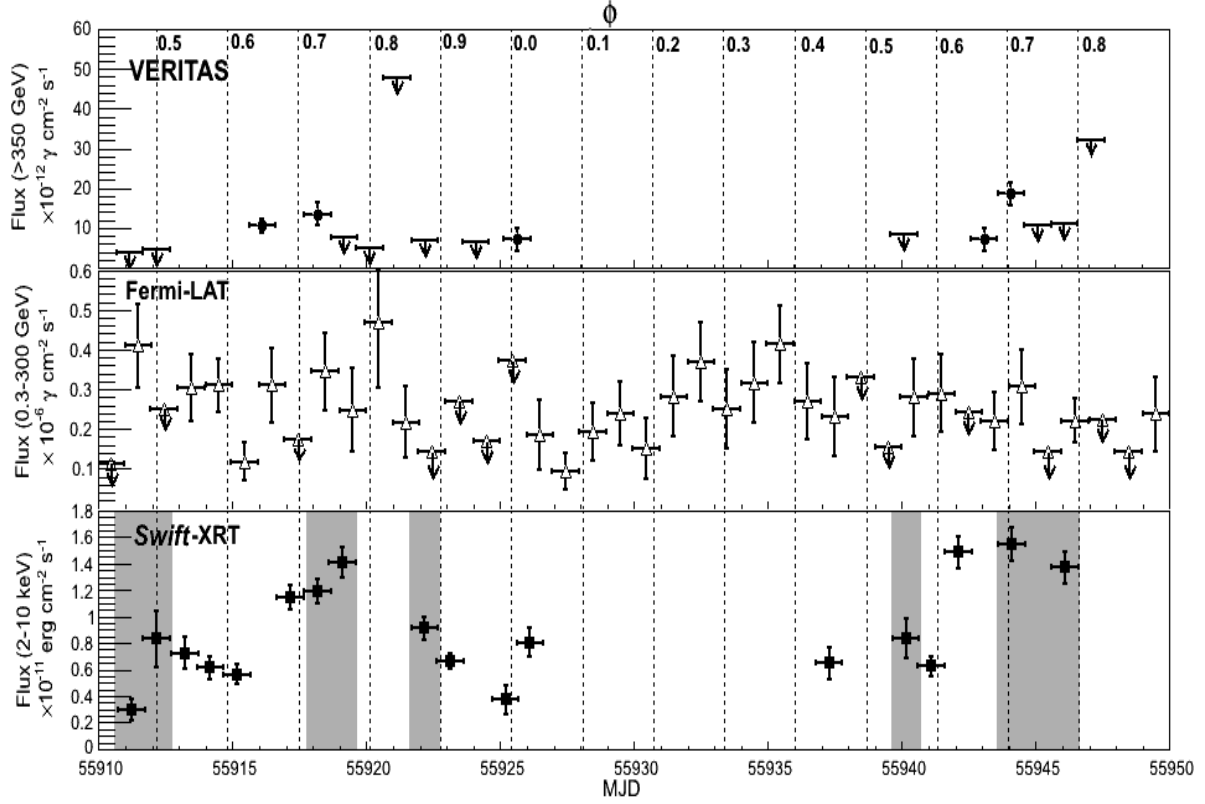


Fig. 1.— The VERITAS (>350 GeV daily integrations, top), Fermi-LAT (0.3-300 GeV, middle), and Swift-*XRT* (0.3-10 keV, bottom) light curves for LS I +61° 303 during December 2011 - February 2012. The data is also shown as a function of orbital phase (ϕ). VERITAS 99% flux upper limits are shown for points with $< 3\sigma$ significance and are represented by arrows. Fermi-LAT upper limits (90% confidence level) are also shown by arrows. The grey shaded regions represent the observations obtained simultaneously which are used for the X-ray/TeV correlation studies in this work.

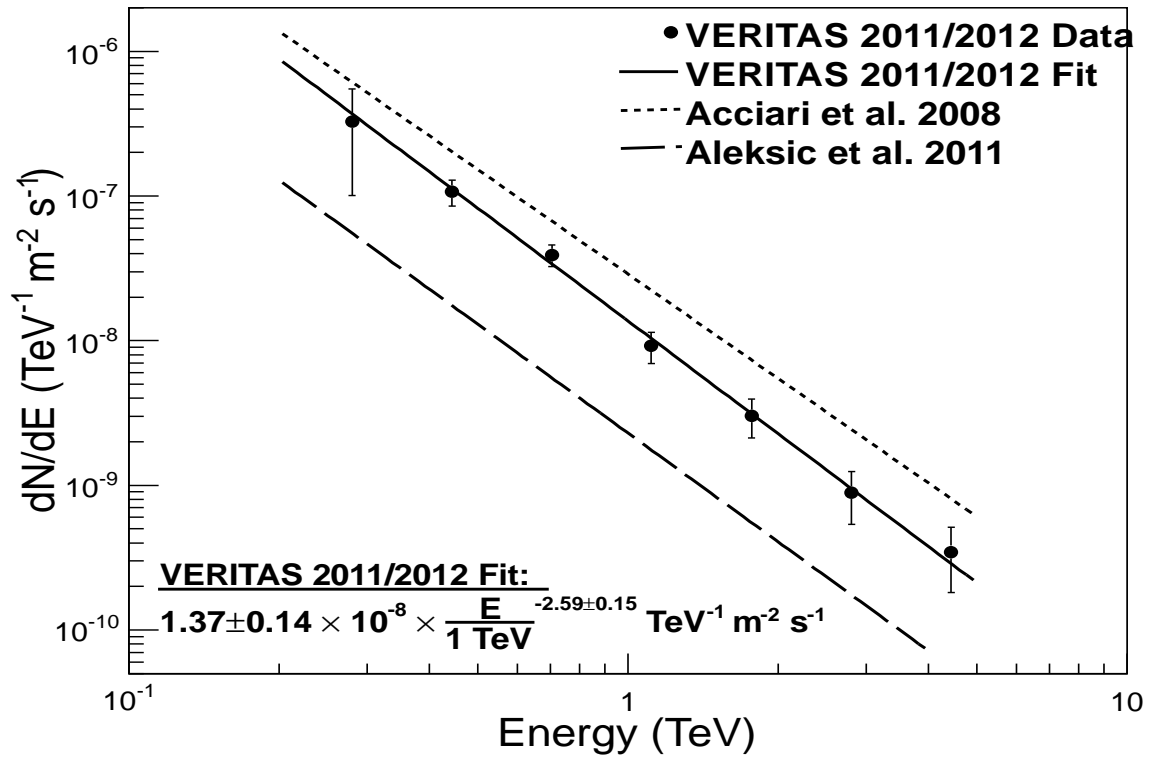


Fig. 2.— The VERITAS SED obtained from the 2011/2012 observations. We also show the SED power-law fit to both higher (Acciari et al. 2008) and lower (Aleksic et al. 2012) flux states of the source.

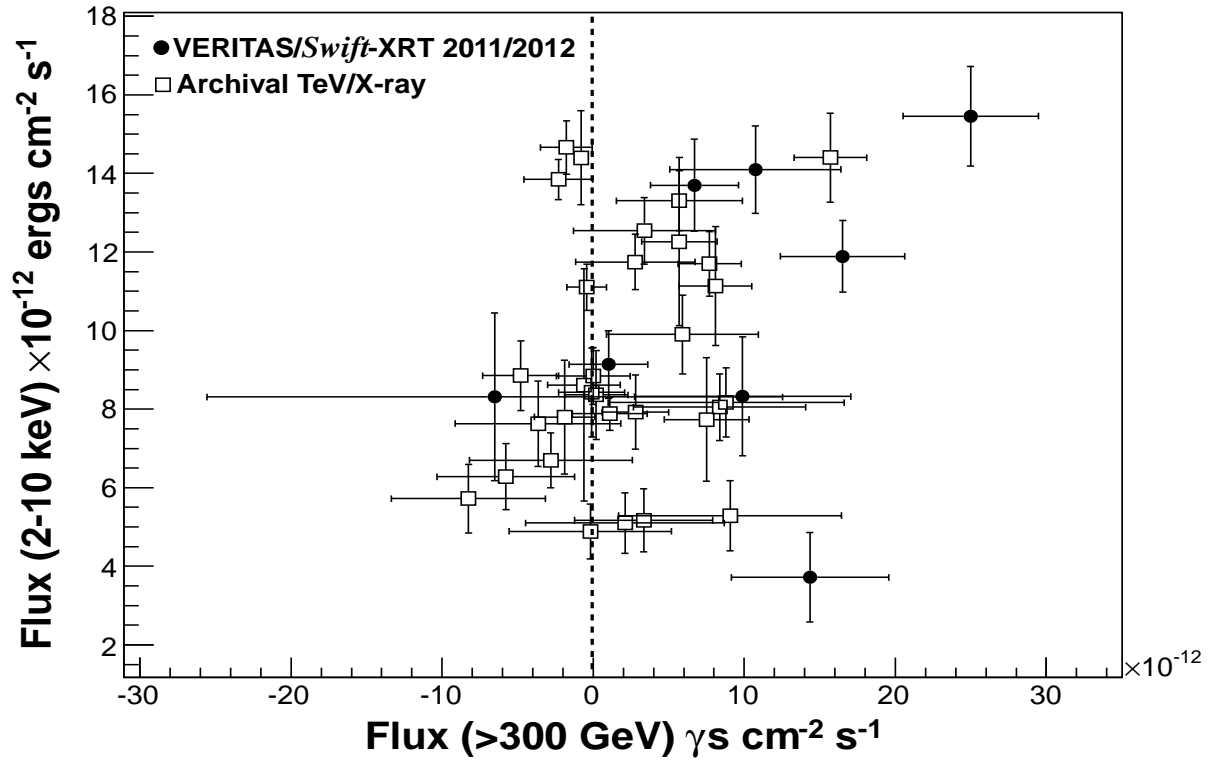


Fig. 3.— The comparison of the strictly simultaneous Swift-XRT and VERITAS data points. The data shows a correlation coefficient of 0.36 ± 0.32 , consistent with two uncorrelated data sets.

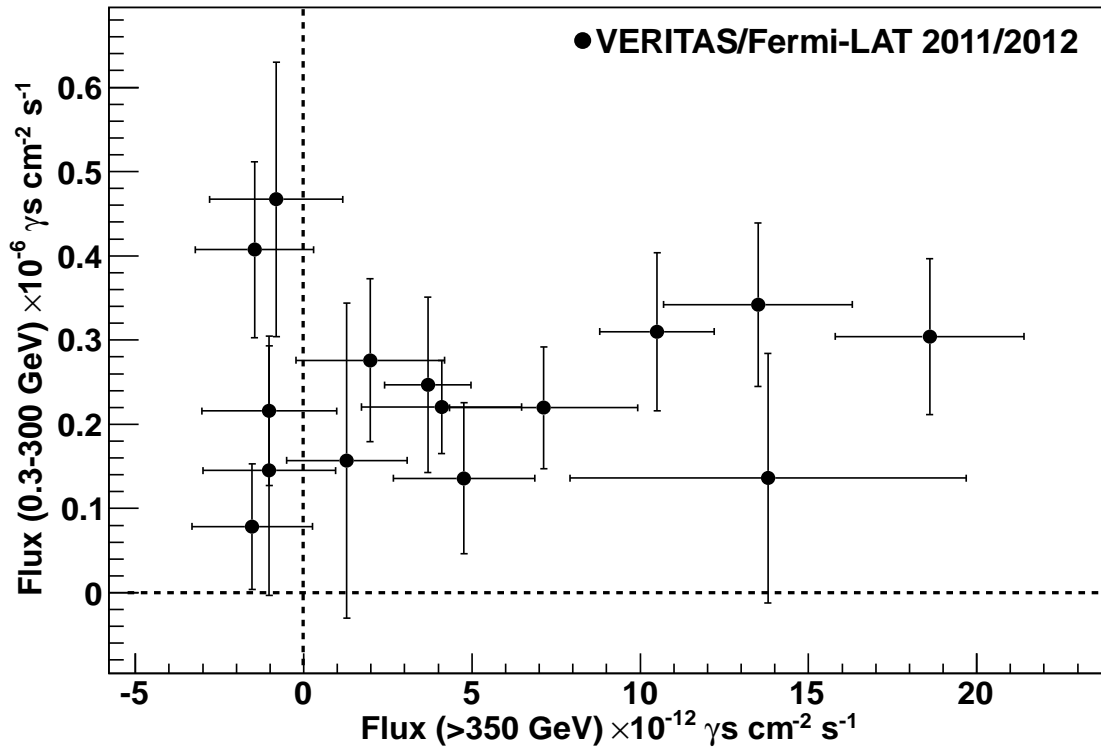


Fig. 4.— The comparison of nightly VERITAS and Fermi-LAT flux points. Analysis of the data results in a correlation coefficient of 0.1 ± 0.3 , consistent with two independent data sets.

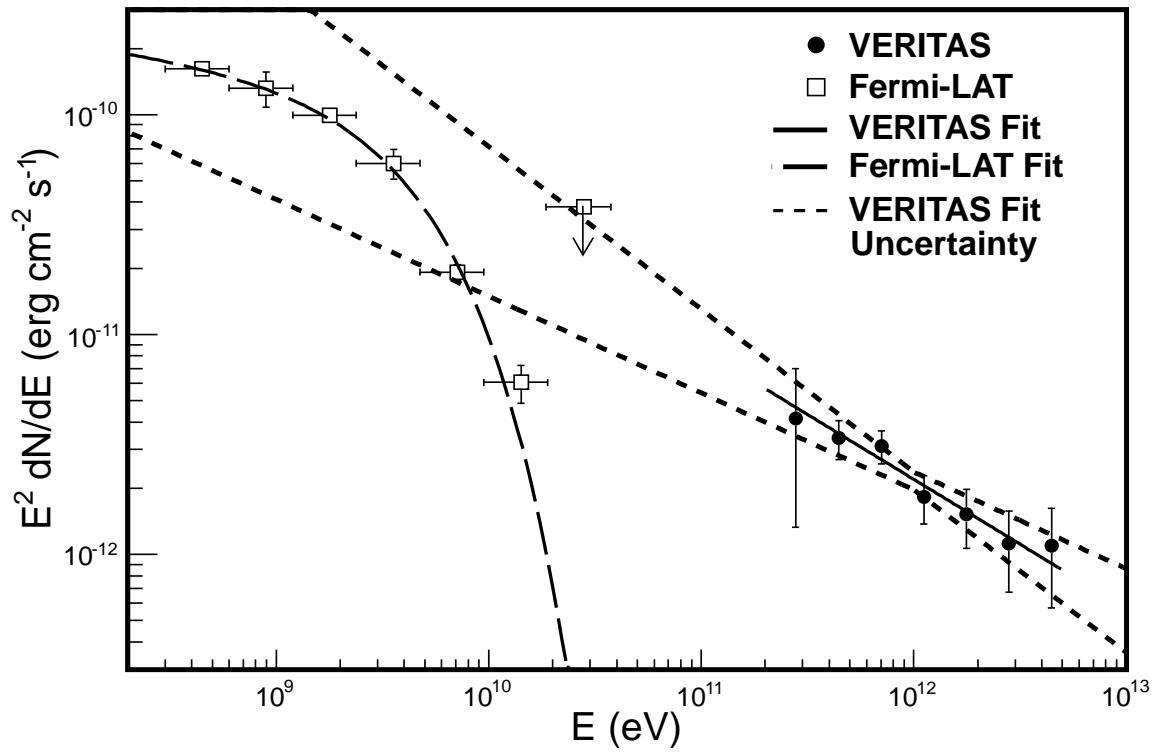


Fig. 5.— The VERITAS and Fermi-LAT spectral energy distribution.